Analysis of High-Speed Interconnects in the Presence of Electromagnetic Interference

Roni Khazaka, *Student Member, IEEE*, and Michel Nakhla, *Fellow, IEEE*

***Abstract*— This paper describes an efficient algorithm based on moment-matching techniques for simulation of high-speed circuits in the presence of electromagnetic interference (EMI). The proposed method is based on the recently developed complex frequency hopping (CFH) technique for interconnect analysis. The new technique is useful for susceptibility analysis and is two to three orders of magnitude faster than conventional simulation techniques. In addition, it can be extended to the analysis of interconnects with frequency-dependent parameters and nonlinear terminations.**

***Index Terms*—Circuit simulation, complex frequency hopping, electromagnetic compatibility, electromagnetic interference, interconnects, moment-matching techniques.**

I. Introduction

THE CURRENT trend toward more complex designs, higher operating frequencies, sharper rise times, shrinking device sizes, low power consumption, and increasing integration of analog circuits with digital blocks has made signal-integrity analysis a challenging task. In addition, electrically long interconnects function as spurious antennas to pick up emissions from other nearby electronic systems [1]. This makes susceptibility to emissions a major concern to current system designers of high-frequency products [2]. Hence, the availability of interconnect simulation tools, including the effect of incident fields, is becoming an important design requirement.

Incident-field coupling to transmission lines have been a problem of interest for many years. Various modeling approaches are possible, the most common one being an extension to the telegrapher's equations [3]–[6]. This approach conserves the quasi-TEM assumption, and models the incident-field effects as distributed sources along the transmission lines. Various publications have addressed the solution of the transmission-line equations in the presence of incident fields [3]–[12]. In general, current simulation techniques rely on solving the system equations at each frequency point to obtain the frequency response, and on convolution to obtain the time-domain response of systems with nonlinear terminations. For large systems, these techniques could be very expensive in terms of central processing unit (CPU) time and memory requirements.

In addition to the electromagnetic interference (EMI) problems of interconnects, other interconnect effects such as delay, ringing, and crosstalk represent critical factors in high-frequency system design, and several authors have studied these effects and proposed simulation techniques [13]–[20]. Recently, model-reduction techniques [21]–[32] such as complex frequency hopping (CFH) have proven to be efficient and reliable techniques for interconnect analysis, providing 100 to 1000 times speed-up over conventional simulation methods, and suited for VLSI and printed circuit board (PCB) designs where a large number of interconnects has to be considered. CFH is a moment-matching technique based on approximating the frequency response of a large linear subnetwork using multipoint Padé expansions, which requires the solution of the network equations at very few frequency points. In addition, CFH provides (through macromodeling [27], [32]) an accurate and efficient link to nonlinear simulators without the need to use computationally expensive convolution techniques. CFH has been applied to networks containing lumped elements and lossy coupled transmission lines [29] with frequency-dependent parameters [30] and nonlinear terminations [27], [32].

This paper presents a technique for the simulation of transmission lines excited by incident fields. Based on CFH, the proposed technique takes full advantage of the benefits outlined earlier. The transmission-line model derived from the modified telegrapher's equations is used to account for the incident fields. A generalized stamp that includes EMI effects in a form suitable for moment-matching techniques is derived, as well as a new moment-generation algorithm for transmission lines excited by incident fields. The proposed technique provides a speed-up of one to two orders of magnitudes over conventional methods for a reasonable accuracy.

This paper is organized as follows. In Section II, an EMI-based interconnect stamp suitable for moment generation is presented. Section III briefly outlines the formulation of the equations representing an arbitrarily large network in the presence of EMI. Section IV outlines the CFH algorithm, and presents new moment-generation algorithms for EMI-based transmission-line models. Some important special cases are presented in Section V, and a summary of the algorithm is presented in Section VI. Numerical results which demonstrate the accuracy and efficiency are given in Section VII.

II. Transmission-Line EMI Stamp

The common approach for analysis of interconnects excited by incident fields is to model them as multiconductor transmission lines with additional distributed sources due to EMI [3]–[6]. The telegrapher's equations are, therefore, modified

Manuscript received February 18, 1997; revised April 7, 1998.

The authors are with the Department of Electronics, Carleton University, Ottawa, Ont., Canada K1S 5B6.

Publisher Item Identifier S 0018-9480(98)04958-8.

to include extra terms representing the distributed sources [1]. Various techniques have been proposed for the solution of the modified telegrapher's equations, both in the time and frequency domain [3]–[12]. In this section, we will present an efficient method for formulating the transmission-line stamp of interconnects illuminated by incident fields. The computed stamp is in a form suitable for simulators based on moment-matching techniques [31]. The advantage of this approach is that it allows efficient simulation of large networks with a large number of lumped and distributed components and interconnects affected by EMI, while benefiting from the CPU speed-up gained from moment-matching techniques.

A. Transmission-Line Equations

The transmission-line equations in the presence of radiated interference can be written in the frequency domain as [1]

$$\frac{d}{dz}\begin{bmatrix}\boldsymbol{V}(z,s)\\ \boldsymbol{I}(z,s)\end{bmatrix} = -(\boldsymbol{D}+s\boldsymbol{E})\begin{bmatrix}\boldsymbol{V}(z,s)\\ \boldsymbol{I}(z,s)\end{bmatrix} + \boldsymbol{F}(z,s) \tag{1}$$

where

$$\boldsymbol{D} = \begin{bmatrix}0 & \boldsymbol{R}\\ \boldsymbol{G} & 0\end{bmatrix} \quad \boldsymbol{E} = \begin{bmatrix}0 & \boldsymbol{L}\\ \boldsymbol{C} & 0\end{bmatrix} \tag{2}$$

and

$$\boldsymbol{F}(z,s) = \begin{bmatrix}\boldsymbol{V}_F\\ \boldsymbol{I}_F\end{bmatrix}. \tag{3}$$

$\boldsymbol{R}$, $\boldsymbol{L}$, $\boldsymbol{C}$, and $\boldsymbol{G}$ are the per u unit length resistance, inductance, capacitance, and conductance matrices, respectively. $\boldsymbol{V}$ and $\boldsymbol{I}$ are the total voltages and currents along the transmission line. $\boldsymbol{V}_F$ and $\boldsymbol{I}_F$ are the equivalent distributed voltage and current sources due to the presence of interference, and are given in terms of the incident electric and magnetic fields by (4) and (5), shown in at the bottom of this page [1], [10], where

$$\boldsymbol{Y}_{TL} = \boldsymbol{G} + s\boldsymbol{C} \tag{6}$$

and $\mathcal{E}_t^i$ and $\mathcal{B}_n^i$ are the transverse and normal components of the incident electric and magnetic fields, respectively, as shown in Fig. 1.

B. Transmission-Line Stamp

The transmission-line stamp is derived from the solution of Telegrapher's equations. In this section, we will present the solution of the transmission-line equations, including distributed sources due to incident fields, and put it in a form suitable for moment-matching techniques. The solution of (1) can be written as

$$\begin{bmatrix}\boldsymbol{V}(l)\\ \boldsymbol{I}(l)\end{bmatrix} = e^{-\varphi l}\begin{bmatrix}\boldsymbol{V}(0)\\ \boldsymbol{I}(0)\end{bmatrix} + e^{-\varphi l}\int_0^l e^{\varphi z}\boldsymbol{F}(z)\,dz \tag{7}$$

where l is the length of the line, and

$$\varphi = \boldsymbol{D} + s\boldsymbol{E}. \tag{8}$$

The lumped sources due to EMI can then be expressed using (7) as

$$\boldsymbol{b}(s) = e^{-\varphi l}\int_0^l e^{\varphi z}\boldsymbol{F}(z)\,dz. \tag{9}$$

In order to derive a stamp that is consistent with moment-matching techniques, the moments of $\boldsymbol{b}(s)$ in (9) and the moments of $e^{-\varphi l}$ in (7) are needed. The latter can be accurately determined using the matrix exponential method [29]. The moments of $\boldsymbol{b}(s)$ will be discussed in Section IV.

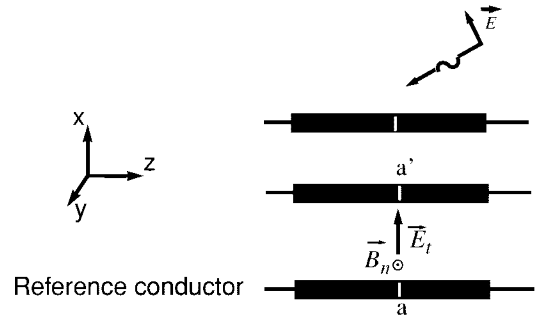

Fig. 1. Transmission lines excited by incident fields.

C. Transmission-Line Stamp With Incident Plane Waves

In this section, the general formulation in (9) will be simplified for transmission lines excited by a uniform plane wave. This approach presents a good approximation for cases where the simulated system is in the far field of the interference source [1]. A frequency-domain representation of an incident uniform plane wave is given by [10], [33]

$$\mathcal{E}^i = \mathcal{E}_o(e_x\hat{a}_x + e_y\hat{a}_y + e_z\hat{a}_z)e^{-j\beta_x x}e^{-j\beta_y y}e^{-j\beta_z z} \tag{10}$$

where

$$e_x = \sin\theta_E\sin\theta_p \tag{11a}$$

$$e_y = -\sin\theta_E\cos\theta_p\cos\phi_p - \cos\theta_E\sin\phi_p \tag{11b}$$

$$\boldsymbol{V_F}(z,s) = s\begin{bmatrix}\cdots\\ \int_a^{a'}(\vec{\mathcal{B}}_n^i)\,dl\\ \cdots\end{bmatrix} = \frac{\partial}{\partial z}\begin{bmatrix}\cdots\\ \int_a^{a'}\vec{\mathcal{E}}_t^i\cdot dl\\ \cdots\end{bmatrix} + \begin{bmatrix}\cdots\\ \{\mathcal{E}_z(\text{conductor } k, z) - \mathcal{E}_z(\textit{reference}\text{ conductor}, z)\}\\ \cdots\end{bmatrix} \tag{4}$$

$$\boldsymbol{I_F}(z,s) = -\boldsymbol{G}\begin{bmatrix}\cdots\\ \int_a^{a'}\vec{\mathcal{E}}_t^i\cdot dl\\ \cdots\end{bmatrix} - s\boldsymbol{C}\begin{bmatrix}\cdots\\ \int_a^{a'}\vec{\mathcal{E}}_t^i\cdot dl\\ \cdots\end{bmatrix} = -\boldsymbol{Y}_{TL}\begin{bmatrix}\cdots\\ \int_a^{a'}\vec{\mathcal{E}}_t^i\cdot dl\\ \cdots\end{bmatrix} \tag{5}$$

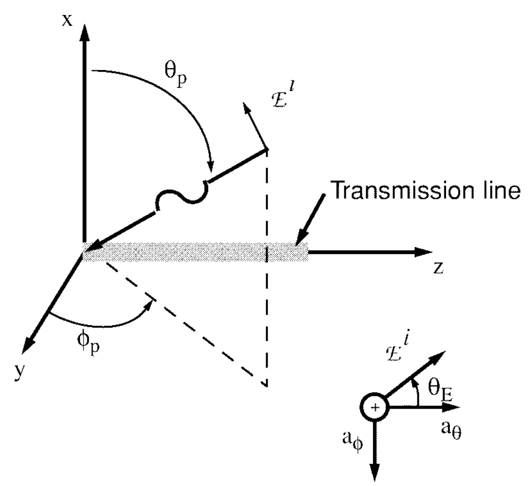

Fig. 2. Incident electromagnetic (EM) field.

$$e_z = -\sin\theta_E \cos\theta_p \sin\phi_p + \cos\theta_E \cos\phi_p \quad (11c)$$

$$\beta_x = -\beta\cos\theta_p \quad (12a)$$

$$\beta_y = -\beta\sin\theta_p\cos\phi_p \quad (12b)$$

$$\beta_z = -\beta\sin\theta_p\sin\phi_p. \quad (12c)$$

The angles θ_E, θ_p, and ϕ_p are shown in Fig. 2. For the case of a uniform plane wave, the forcing function $\boldsymbol{F}(z, s)$ defined in (3) can be reduced as shown in (13), at the bottom of this page, where

$$\psi_k = \frac{\beta_x x_k + \beta_y y_k}{2} \quad (14)$$

and, x_k and y_k are the coordinates of transmission line k. In the case of uniform plane-wave excitation, the dependence of $\boldsymbol{F}(z, s)$ on z can be reduced to an exponential in the form

$$\boldsymbol{F}(z, s) = \Gamma(s)e^{-j\beta_z z}. \quad (15)$$

Therefore, the additional sources due to distributed voltages and currents on the transmission line can be expressed as a product of three different functions of s as

$$\boldsymbol{b}(s) = \boldsymbol{T}(s)\boldsymbol{Q}(s)\Gamma(s) \quad (16)$$

and $\boldsymbol{T}(s)$, $\boldsymbol{Q}(s)$, and $\Gamma(s)$, shown in (17) and (18), at the bottom of this page.

The transmission-line stamp (7), (16) developed in this section is in a form suitable for implementation in moment-matching techniques. In the following sections, this stamp is included in the general formulation of circuit equations of an arbitrarily large network.

III. Network Equations in the Presence of EMI

Consider a linear network ϕ which contain linear lumped components and N_t lossy coupled transmission-line sets, with n_k coupled conductors in transmission-line set k. Assume the network ϕ has N_ϕ nodal variables, the frequency-domain modified nodal admittance (MNA) matrix [22] equations for the network in the presence of incident field excitation can be formulated as

$$\boldsymbol{Y}(s)\boldsymbol{X}(s) = \Psi(s) \quad (19)$$

or

$$\begin{bmatrix} \boldsymbol{H}_\phi + s\boldsymbol{W}_\phi & \boldsymbol{D}_1 & \cdots & \boldsymbol{D}_{N_t} \\ \boldsymbol{A}_1\boldsymbol{D}_1^t & \boldsymbol{B}_1 & 0 & 0 \\ \cdots & 0 & \cdots & 0 \\ \boldsymbol{A}_{N_t}\boldsymbol{D}_{N_t}^t & 0 & 0 & \boldsymbol{B}_{N_t} \end{bmatrix} \begin{bmatrix} \boldsymbol{V}(s) \\ \boldsymbol{I}_1(s) \\ \cdots \\ \boldsymbol{I}_{N_t}(s) \end{bmatrix} = \begin{bmatrix} \boldsymbol{e}_\phi(s) \\ \boldsymbol{b}_1(s) \\ \cdots \\ \boldsymbol{b}_{N_t}(s) \end{bmatrix} \quad (20)$$

where

$\boldsymbol{V}_\phi(s) \in C^{N_\phi}$ vector of the N_ϕ variables describing the subnetwork ϕ, which includes the Laplace-domain node voltages, appended by currents through independent voltage sources and linear inductors;

$\boldsymbol{W}_\phi \in \Re^{N_\phi \times N_\phi}$ constant matrices describing the lumped memory and memoryless elements;

$\boldsymbol{H}_\phi \in \Re^{N_\phi \times N_\phi}$ of network ϕ, respectively;

$\boldsymbol{e}_\phi \in C^{N_\phi}$ represents the lumped sources in the system;

$$\boldsymbol{F}(z, s) = \mathcal{E}_o \begin{bmatrix} j\dfrac{\sin\psi_k}{\psi_k} e^{-j\psi_k}[\beta_z(e_x x_k + e_y y_k) - e_z(\beta_x x_k + \beta_y y_k)] \\ \cdots \\ -\boldsymbol{Y}_{TL}\dfrac{\sin\psi_k}{\psi_k} e^{-j\psi_k}(e_x x_k + e_y y_k) \\ \cdots \end{bmatrix} e^{-j\beta_z z} \quad (13)$$

$$\begin{aligned} \boldsymbol{T}(s) &= e^{-\varphi l} \\ \boldsymbol{Q}(s) &= \int_0^l e^{\varphi z} e^{-j\beta_z z}\, dz \end{aligned} \quad (17)$$

$$\Gamma(s) = \mathcal{E}_o \begin{bmatrix} j\dfrac{\sin\psi_k}{\psi_k} e^{-j\psi_k}[\beta_z(e_x x_k + e_y y_k) - e_z(\beta_x x_k + \beta_y y_k)] \\ \cdots \\ -\boldsymbol{Y}_{TL}\dfrac{\sin\psi_k}{\psi_k} e^{-j\psi_k}(e_x x_k + e_y y_k) \\ \cdots \end{bmatrix} \quad (18)$$

$\boldsymbol{D}_k = [d_{i,j}]$ with elements $d_{i,j} \in \{0, 1\}$ and with $i \in \{1, 2, \cdots, N_\phi\}$, $j \in \{1, 2, \cdots, 2n_k\}$ with a maximum of one nonzero in each row or column, is a selector matrix that maps $\boldsymbol{I}_k(s) \in C^{2n_k}$, the vector of currents entering the transmission-line subnetwork k, into the node space C^{N_ϕ} of the network ϕ;

$\boldsymbol{b}_k(s) \in C^{2n_k}$ represents the effect of interference on transmission-line set k;

$\boldsymbol{A}_k$ and $\boldsymbol{B}_k$ relate the terminal voltages $\boldsymbol{V}_k$ and currents $\boldsymbol{I}_k$ of transmission-line set k by the following expression:

$$\boldsymbol{A}_k\boldsymbol{V}_k + \boldsymbol{B}_k\boldsymbol{I}_k = \boldsymbol{b}_k \tag{21}$$

where $\boldsymbol{b}_k$ is given by (16).

Conventional simulation techniques rely on solving (20) at a large number of frequency points to obtain the frequency response. The time-domain response is then calculated using inverse fast Fourier transform (IFFT) for linear terminations, and using convolution in case of nonlinear terminations. This approach has two main disadvantages. First, the CPU cost of solving the network equations at many frequency points could be very high due to the large number of lower/upper (L/U) triangular matrix decompositions (one per frequency point). Secondly, for nonlinear terminations, the convolution increases the CPU and memory requirements [38] and can introduce numerical instability. However, these problems can be avoided by using CFH [29]. CFH has been applied to lossy distributed transmission-line networks [31] with frequency-dependent parameters [30] and nonlinear terminations [27], [32]. In Section IV, a technique based on CFH is developed for the simulation of interconnects excited by incident fields.

IV. CFH and Moment Calculation in the Presence of Incident EM Fields

The CFH technique is fast and accurate, and naturally lends itself to the simulation of systems with nonlinear terminations through time-domain macromodels [32]. In this section, we will present a brief overview of moment-matching techniques, and describe a new approach that allows the simulation of systems in the presence of EMI.

A. Overview of Moment-Matching Techniques

Moment matching is a model-reduction technique, whereby the Taylor series expansion of the network equations is used to generate a low-order transfer function approximation. CFH extends the process to multiple expansion points in the complex plane near or on the imaginary axis, in order to insure the accuracy of the approximation for the complete frequency range of interest. A Taylor series expansion of $\boldsymbol{X}(s)$ in (19) around a complex frequency s_o can be written as

$$\boldsymbol{X}(s) = \sum_n \boldsymbol{M}_n(s - s_o)^n \tag{22}$$

where $\boldsymbol{M}_n$ are the moments of the system and s_o is the expansion point of the CFH algorithm. Padé approximation is then used on (22) to obtain a low-order rational transfer function for the system, which can be used to evaluate the frequency response of the network, and to compute its poles and residues to obtain the transient response [31].

Finally, the coefficients of the transfer function are obtained from the system moments using Padé approximation [31], [35], [36]. A search algorithm and an efficient method for the extraction of the poles of the system can be found in [29]. The algorithm provides a method for the selection and minimization of optimum expansion points, as well as a technique for combining the information obtained from each expansion. An alternative approach, Padé Via Lanczos [37], overcomes the numerical ill conditioning encountered by direct Padé approximation, but is limited to systems described by a set of ordinary differential equations. In this paper, the CFH technique was chosen since it can handle distributed transmission lines without the need to discretize the partial differential equations in the spatial domain.

It is to be noted that the main reason behind the efficiency of the CFH algorithm is that it requires one L/U decomposition of the matrix $\boldsymbol{Y}$ per frequency hop, whereas conventional simulation techniques (e.g., IFFT or time stepping) require one L/U decomposition for each frequency or time point. Generally, the number of frequency hops (around two to ten) is far less than the number of frequency/time points required to get an accurate solution. The following sections will focus on the calculation of the system moments for circuits containing transmission lines excited by incident waves.

B. Calculation of System Moments in the Presence of EMI

Calculation of the system moments $\boldsymbol{M}_n$ defined in (22) is required at each frequency hop in the CFH algorithm. A recursive equation for the evaluation of these moments at a particular frequency s_0 can be obtained in the form

$$\boldsymbol{Y}(s_o)\boldsymbol{M}_0 = \Psi_0 \tag{23}$$

$$\boldsymbol{Y}(s_o)\boldsymbol{M}_n = -\sum_{r=1}^{n} \frac{\left.\dfrac{\partial^r}{\partial s^r}\boldsymbol{Y}(s)\right|_{s=s_o} \boldsymbol{M}_{n-r}}{r!} + \Psi_n \tag{24}$$

where the derivatives $\boldsymbol{Y}^{(r)}(s)$ are obtained in terms of the lumped components and the moments of the hybrid parameters of the transmission line, which are calculated using the matrix exponential method [31]. The coefficients Ψ_n are derived from the moments of the sources due to EMI $(\boldsymbol{b}(s))$. The evaluation of these coefficients is covered in detail in the following section.

C. Transmission-Line Moments in the Presence of EMI

The transmission-line stamp is expressed in terms of the moments of the sources $\boldsymbol{b}(s)$ due to EMI for each of the transmission lines affected, as well as the moments of the transmission-line hybrid parameters. As shown in Section II, in the case of incident plane waves, the transmission-line stamp is expressed as

$$\begin{bmatrix}\boldsymbol{V}(l)\\ \boldsymbol{I}(l)\end{bmatrix} = \boldsymbol{T}(s)\begin{bmatrix}\boldsymbol{V}(0)\\ \boldsymbol{I}(0)\end{bmatrix} + \boldsymbol{b}(s) \tag{25}$$

where

$$\boldsymbol{b}(s) = \boldsymbol{T}(s)\boldsymbol{Q}(s)\Gamma(s) \tag{26}$$
$$\boldsymbol{T}(s) = e^{-\varphi l} \tag{27}$$
$$\boldsymbol{Q}(s) = \int_0^l e^{\boldsymbol{H}z}\, dz \tag{28}$$
$$\boldsymbol{H} = \varphi - \boldsymbol{K}s = \boldsymbol{H}_0 + \boldsymbol{H}_1 s \tag{29}$$
$$\boldsymbol{K} = \frac{\sqrt{\varepsilon_r \mu_r}}{c}\boldsymbol{U}\sin\theta_p \sin\phi_p \tag{30}$$

where φ is defined in (8), θ_p and ϕ_p are defined in Fig. 2, $\boldsymbol{U}$ is the unity matrix, and c is the speed of the light in vacuum. The moments of $\boldsymbol{b}(s)$ are defined in terms of $\boldsymbol{T}_i$, $\boldsymbol{Q}_j$, and Γ_k, the moments of $\boldsymbol{T}(s)$, $\boldsymbol{Q}(s)$, and $\Gamma(s)$, respectively,

$$\boldsymbol{b}_k = \sum_i \sum_j \boldsymbol{T}_i \boldsymbol{Q}_j \Gamma_{k-i-j}. \tag{31}$$

The moments of $\boldsymbol{T}(s)$ are calculated using the matrix exponential method [29], the moments of $\Gamma(s)$ are obtained from (18) (examples are shown in Section V). Finally, the following recursive formulas can be derived for the calculation of the moments of $\boldsymbol{Q}(s)$:

$$\boldsymbol{H}_0\boldsymbol{Q}_0 = \Delta_0 \tag{32}$$
$$\boldsymbol{H}_0\boldsymbol{Q}_i = -\boldsymbol{H}_1\boldsymbol{Q}_{i-1} + \Delta_i. \tag{33}$$

The coefficients Δ_i are determined as follows:

$$\Delta(s) = e^{(\boldsymbol{H}_0+\boldsymbol{H}_1 s)l} - \boldsymbol{U} = \boldsymbol{P}(s) - \boldsymbol{U} = \sum_i \boldsymbol{P}_i s^i - \boldsymbol{U} \tag{34}$$

where $\boldsymbol{U}$ is the unity matrix, and coefficients $\boldsymbol{P}_i$ can be recursively obtained as follows:

$$\boldsymbol{P}_i = \sum_{j=1}^{\infty} \boldsymbol{P}_{i,j} \tag{35}$$

where $\boldsymbol{P}_{i,j}$ are given recursively by

$$\boldsymbol{P}_{0,j} = \frac{\boldsymbol{H}_0\boldsymbol{P}_{0,j-1}l}{j} \qquad (j > 1) \tag{36}$$
$$\boldsymbol{P}_{i,j} = \frac{(\boldsymbol{H}_0\boldsymbol{P}_{i,j-1} + \boldsymbol{H}_1\boldsymbol{P}_{i-1,j})l}{i+j} \tag{37}$$

where l is the length of the transmission line and

$$\boldsymbol{P}_{0,0} = \boldsymbol{U} \tag{38}$$
$$\boldsymbol{P}_{i,-1} = \boldsymbol{0}. \tag{39}$$

The ∞ in (35) is only a formality of description. In general, only about 20–30 terms are needed if the eigenvalues of $\boldsymbol{H}l$ are inside the unit circle in the complex plane at the highest frequency. For electrically long lines, the eigenvalues will be outside the unit circle, and the line can be efficiently divided into subsections by noting that

$$e^{\boldsymbol{H}l} = e^{\boldsymbol{H}(l/2)}e^{\boldsymbol{H}(l/2)} \tag{40}$$

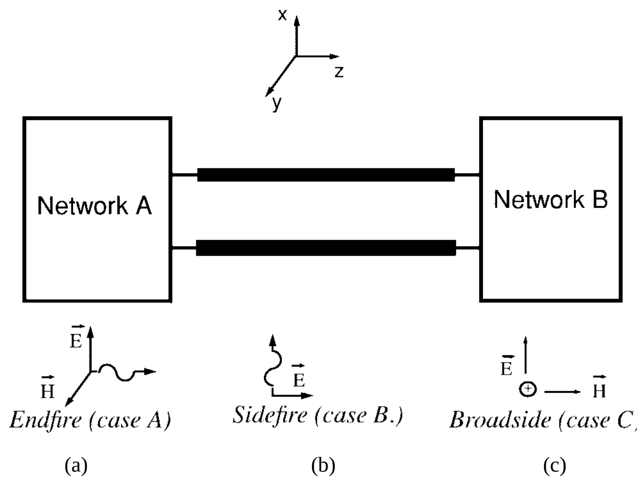

Fig. 3. Special cases.

which implies that the moments of a line can be generated by squaring the half-line moments. If $\boldsymbol{P}_n^{(1/2)}$ represents the half-line moments, and $\boldsymbol{P}_n$ the full-line moments, then

$$\boldsymbol{P}_n = \sum_{i=1}^{n} \boldsymbol{P}_i^{(1/2)}\boldsymbol{P}_{n-i}^{(1/2)}. \tag{41}$$

Using this technique, the line can be subdivided by a power of two and the moments of the smallest section calculated.

D. Summary of the Calculations of the Source Moments

In this section, a summary of the steps involved in the calculations of the moments of the incident sources $\boldsymbol{b}(s)$ is given below.

Step 1: Determine the coefficients $\boldsymbol{P}_i$ associated with the transmission line using (37)–(41).
Step 2: Determine the coefficients Δ_i using (34).
Step 3: Determine the moments of $\boldsymbol{Q}(s)$ using (32) and (33).
Step 4: Determine the moments of $\boldsymbol{T}(s)$ using the matrix exponential technique [29].
Step 5: Determine the moments of $\Gamma(s)$ (see examples in Section V).
Step 6: Determine the moments of $\boldsymbol{b}(s)$ using (31).

V. Special Cases

In this section, we will consider some important special cases presented in [1] (endfire, sidefire, and broadside excitation), in order to illustrate the procedures described in the previous sections.

A. Endfire Excitation

For endfire excitation [see Fig. 3(a)], the forcing function $\boldsymbol{F}(s, z)$ becomes

$$\boldsymbol{F}(s,z) = \begin{bmatrix} -\mathcal{E}_o d\,\dfrac{\sqrt{\varepsilon_r\mu_r}}{c}\,s \\ -\boldsymbol{Y}_{TL}\mathcal{E}_o d \end{bmatrix} e^{-(\sqrt{\varepsilon_r\mu_r}/c)sz} \tag{42}$$

where d is the distance between the lines and c is the speed of light. The moments of $\boldsymbol{b}(s)$ can then be calculated as

$$\boldsymbol{b}(s) = e^{-\varphi l}\boldsymbol{Q}(s)\begin{bmatrix} -\mathcal{E}_o d \dfrac{\sqrt{\varepsilon_r \mu_r}}{c} s \\ -\boldsymbol{Y}_{TL}\mathcal{E}_o d \end{bmatrix} \tag{43}$$

where the moments of $e^{-\varphi l}$ are calculated using the matrix exponential method [29], and $\boldsymbol{Q}(s)$ is obtained from (32) and (33) with

$$\boldsymbol{H}(s) = \boldsymbol{H}_0 + \boldsymbol{H}_1 s = \boldsymbol{D} + s\left(\boldsymbol{E} - \frac{\sqrt{\varepsilon_r \mu_r}}{c}\boldsymbol{U}\right). \tag{44}$$

$\boldsymbol{D}$ and $\boldsymbol{E}$ are defined in (2). The moments of $\Gamma(s)$ are obtained from

$$\Gamma(s) = \begin{bmatrix} 0 \\ -\boldsymbol{G}\mathcal{E}_o d \end{bmatrix} + \begin{bmatrix} -\mathcal{E}_o d \dfrac{\sqrt{\varepsilon_r \mu_r}}{c} \\ -\boldsymbol{C}\mathcal{E}_o d \end{bmatrix} s. \tag{45}$$

The moments of $\boldsymbol{b}(s)$ are then obtained using (31).

B. Sidefire Excitation

Similarly, for sidefire excitation [see Fig. 3(b)], $\boldsymbol{b}(s)$ simplifies to

$$\boldsymbol{b}(s) = e^{-\varphi l}\boldsymbol{Q}(s)\begin{bmatrix} -j\mathcal{E}_o \beta d \dfrac{\sin \beta d/2}{\beta d/2} e^{-j(\beta d/2)} \\ 0 \end{bmatrix}. \tag{46}$$

$\boldsymbol{Q}(s)$ is obtained from (32) and (33) with

$$\boldsymbol{H}(s) = \boldsymbol{H}_0 + \boldsymbol{H}_1 s = \boldsymbol{D} + s\boldsymbol{E}. \tag{47}$$

C. Broadside Excitation

Finally, for broadside excitation [see Fig. 3(c)], $\boldsymbol{b}(s)$ can be expressed as

$$\boldsymbol{b}(s) = e^{-\varphi l}\boldsymbol{Q}(s)\Gamma(s) \tag{48}$$

as in the case of sidefire excitation, $\boldsymbol{Q}(s)$ is obtained from (32) and (33) with

$$\boldsymbol{H}(s) = \boldsymbol{H}_0 + \boldsymbol{H}_1 s = \boldsymbol{D} + s\boldsymbol{E}. \tag{49}$$

The frequency derivatives of $\Gamma(s)$ can be easily obtained from

$$\Gamma(s) = \begin{bmatrix} 0 \\ -\boldsymbol{G}\mathcal{E}_o d \end{bmatrix} + \begin{bmatrix} 0 \\ -\boldsymbol{C}\mathcal{E}_o d \end{bmatrix} s. \tag{50}$$

VI. Summary of the System-Simulation Algorithm

The following steps summarize the computational procedure for evaluating the response of a linear network containing distributed transmission lines excited by an incident EM field.

- For a frequency s_o:
  - *Step 1:* Calculate the transmission-line moments $\boldsymbol{T}(s)$ as outlined in [29].
  - *Step 2:* Find the moments of $\boldsymbol{b}(s)$ as outlined in Section IV.
  - *Step 3:* Repeat Steps 1 and 2 for every transmission-line system in the network.
  - *Step 4:* Find the derivatives of $\boldsymbol{Y}(s)$ using the transmission-line moments [29].
  - *Step 5:* Calculate the network moments using (23) and (24).
- Repeat Steps 1–6 at various frequency points according to the binary search algorithm of CFH.
- Use the CFH algorithm [29] to compute the dominant poles of the network and corresponding residues.

The transient response of linear interconnect networks can be obtained analytically from the computed poles and residues. In case of interconnect networks with nonlinear terminations, a time-domain macromodel for the linear subnetwork is derived [32] using the dominant poles and residues. This macromodel takes the form of a set of ordinary differential equations, which can be solved simultaneously with the nonlinear differential equations describing the rest of the network using any of the conventional circuit simulators such as SPICE.

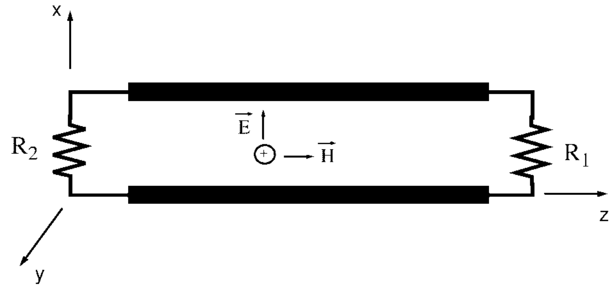

Fig. 4. Two lines excited with an incident field.

VII. Computional Results

A. Example 1

To verify the accuracy of the proposed algorithm, consider the simple example shown in Fig. 4, which consists of a transmission line terminated with resistive loads $R_1 = R_2 = 50\ \Omega$ in the presence of an incident uniform plane wave. The electric field has a 1-V/m amplitude and a 1-ns rise/fall time. The response of this circuit can be evaluated using the analytical solution described in [1].

CFH was applied to this circuit for analysis up to a maximum frequency of 4.5 GHz. The maximum frequency can be estimated based on the input rise time [39]. The number of hops required was two. The time-domain response of this circuit is shown in Fig. 5, which show that the CFH results are consistent with the analytical results. Note that the CFH algorithm requires only one L/U decomposition of the system MNA for each frequency hope (two L/U decomposition in this case). Conventional techniques require one L/U decomposition for each frequency point. For 1000 frequency points, this translates into a speed-up $500:1$.

B. Example 2

To demonstrate the efficiency of the method, a relatively large interconnect network extracted from the layout of an industrial printed circuit board, consisting of 458 resistors, in-

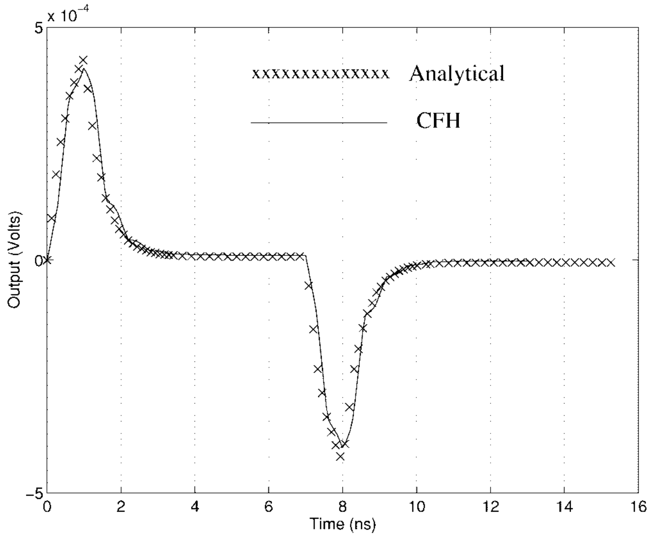

Fig. 5. Time-domain response of circuit in Example 1.

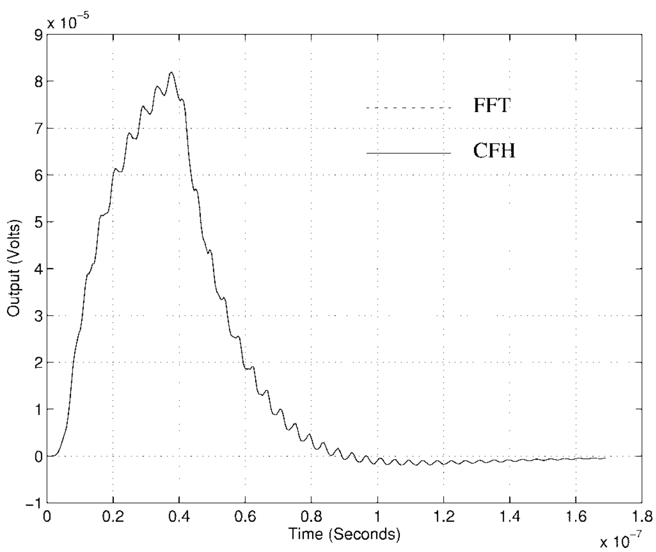

Fig. 6. Time-domain response of circuit in Example 2.

ductors and capacitors, and 12 transmission lines is considered. The incident field is a uniform plane wave with electric field of 1-V/m amplitude and 5-ns rise/fall time. CFH was applied to this circuit for analysis up to 0.6 GHz. *The number of hops required was five*. The algorithm for determining the order of the expansion and the number of hops can be found in [28], [29], and [31]. In Fig. 6, the CFH-generated transient response is compared with the FFT response obtained using 1024 frequency-point solutions and, as seen, the two responses are indistinguishable. It is to be noted that the dominant cost of a frequency hop is the L/U decomposition of the MNA matrix, which is approximately the CPU cost of one frequency-point analysis using conventional techniques [19], [31]. The speed-up ratio obtainable in this example is approximately 200 : 1.

VIII. Conclusion

A method has been developed for the simulation of interconnect networks in the presence of incident EM fields. A new interconnect stamp based on the MNA formulation has been presented, and the CFH algorithm was generalized to handle the new stamp. The proposed technique allows the simulation of the EM immunity of high-speed systems while benefiting from the CPU speed-up generated by the CFH technique. This method can be easily extended to the analysis of nonlinear terminations through macromodeling. This allows the simulation of nonlinear terminations without having to resort to convolution techniques.

References

[1] C. R. Paul, *Analysis of Multiconductor Transmission Lines.* New York: Wiley, 1994.

[2] ——, *Introduction to Electromagnetic Compatibility.* New York: Wiley, 1992.

[3] C. D. Taylor, R. S. Satterwhite, and C. W. Harrison, "The response of a terminated two-wire transmission line excited by a nonuniform electromagnetic field," *IEEE Trans. Antennas Propagat.*, vol. AP-13, pp. 987–989, Nov. 1965.

[4] A. K. Agrawal, H. J. Price, and S. H. Gurbaxani, "Transient response of multiconductor transmission lines excited by a nonuniform electromagnetic field," *IEEE Trans. Electromag. Compat.*, vol. EMC-22, pp. 119–129, May 1980.

[5] A. A. Smith, "A more convenient form of the equations for the response of a transmission line excited by nonuniform fields," *IEEE Trans. Electromag. Compat.*, vol. EMC-15, pp. 151–152, Aug. 1973.

[6] C. R. Paul, "Frequency response of multiconductor transmission lines illuminated by an incident electromagnetic field," *IEEE Trans. Microwave Theory Tech.*, vol. MTT-22, pp. 454–457, Apr. 1976.

[7] I. Wuyts and D. De Zutter, "Circuit model for plane-wave incidence on multiconductor transmission lines," *IEEE Trans. Electromag. Compat.*, vol. 36, pp. 206–212, Aug. 1994.

[8] Y. Kami and R. Sato, "Circuit-concept approach to externally excited transmission lines," *IEEE Trans. Electromag. Compat.*, vol. EMC-27, pp. 177–183, Nov. 1985.

[9] N. Ari and W. Blumer, "Analytic formulation of the response of a two-wire transmission line excited by a plane wave," *IEEE Trans. Electromag. Compat.*, vol. 30, pp. 437–448, Nov. 1988.

[10] C. R. Paul, "Literal solutions for the time-domain response of a two-conductor transmission line excited by an incident electromagnetic field," *IEEE Trans. Electromag. Compat.*, vol. 37, pp. 241–251, May 1995.

[11] F. Schlagenhaufer and H. Singer, "Investigation of field excited multi-conductor lines with nonlinear loads," in *Proc. Int. Symp. Electromagnetic Compatability*, Washington DC, Aug. 1990, pp. 95–99.

[12] P. Bernardi, R. Cicchetti, and C. Pirone, "Transient response of a microstrip line circuit excited by an external electromagnetic source," *IEEE Trans. Electromag. Compat.*, vol. 34, pp. 100–108, May 1992.

[13] W. W. M. Dai, "Special issue on simulation, modeling, and electrical design of high-speed and high-density interconnects," *IEEE Trans. Circuits Syst.*, vol. 39, pp. 857–982, Nov. 1992.

[14] A. R. Djordjević, T. K. Sarkar, and R. F. Harrington, "Analysis of lossy transmission lines with arbitrary nonlinear terminal networks," *IEEE Trans. Microwave Theory Tech.*, vol. MTT-34, pp. 660–666, June 1986.

[15] F. Y. Chang, "The generalized method of characteristics for waveform relaxation analysis of lossy coupled transmission lines," *IEEE Trans. Microwave Theory Tech.*, vol. 37, pp. 2028–2038, Dec. 1989.

[16] J. E. Schutt-Aine and R. Mittra, "Nonlinear transient analysis of coupled transmission lines," *IEEE Trans. Circuits Syst.*, vol. 36, pp. 959–967, July 1989.

[17] R. Wang and O. Wing, "Transient analysis of dispersive VLSI interconnects terminated in nonlinear loads," *IEEE Trans. Computer-Aided Design*, vol. 11, pp. 1258–1277, Oct. 1992.

[18] N. Orhanovic, P. Wang, and V. K. Tripathi, "Generalized method of characteristics for time domain simulation of multiconductor lossy transmission lines," presented at the Proc. IEEE Circuits Systems Symp., New Orleans, LA, May 1990.

[19] T. K. Tang, M. S. Nakhla, and Richard Griffith, "Analysis of lossy multiconductor transmission lines using the asymptotic waveform evaluation technique," *IEEE Trans. Microwave Theory Tech.*, vol. 39, pp. 2107–2116, Dec. 1991.

[20] R. Griffith and M. S. Nakhla, "Mixed frequency/time domain analysis on nonlinear circuits," *IEEE Trans. Computer-Aided Design*, vol. 10, pp. 1032–1043, Aug. 1992.

[21] J. E. Bracken, V. Raghavan, and R. A. Rohrer, "Interconnect simulation with asymptotic waveform evaluation (AWE)," *IEEE Trans. Circuits Syst. I,* vol. 39, pp. 869–878, Nov. 1992.
[22] T. K. Tang and Michel Nakhla, "Analysis of high-speed VLSI interconnects using the asymptotic waveform evaluation technique," *IEEE Trans. Computer-Aided Design,* vol. 11, pp. 341–352, Mar. 1992.
[23] S. Lin and E. S. Kuh, "Transient simulation of lossy interconnects based on recursive convolution formula," *IEEE Trans. Computer-Aided Design,* vol. 39, pp. 879–892, Nov. 1992.
[24] G. J. Burke, E. K. Miller, and S. Chakrabarti, "Using model based parameter estimation to increase the efficiency of computing electromagnetic transfer functions," *IEEE Trans. Magn.,* vol. 25, pp. 2087–2089, July 1989.
[25] S. K. Das and W. T. Smith, "Incident field coupling analysis of multiconductor transmission lines using asymptotic waveform evaluation," in *Proc. IEEE Int. Symp. Electromagnetic Compatability,* Santa Clara, CA, Aug. 1996, pp. 265–270.
[26] R. Khazaka and M. Nakhla, "Analysis of high-speed interconnects in the presence of electromagnetic interference," in *IEEE MTT-S Int. Microwave Symp. Dig.,* San Francisco, CA, June 1996, pp. 1811–1814.
[27] E. Chiprout and M. S. Nakhla, "Fast nonlinear waveform estimation of large distributed networks," in *Proc. IEEE MTT-S Int. Microwave Symp.,* Albuquerque, NM, 1992, pp. 1341–1344.
[28] R. Sanaie, E. Chiprout, M. Nakhla, and Q. J. Zhang, "A fast method for frequency and time domain simulation of high-speed VLSI Interconnects," *IEEE Trans. Microwave Theory Tech.,* vol. 42, pp. 2562–2571, Dec. 1994.
[29] E. Chiprout and M. Nakhla, "Analysis of interconnect networks using complex frequency hopping (CFH)," *IEEE Trans. Computer-Aided Design,* vol. 14, pp. 186–200, Feb. 1995.
[30] R. Khazaka, E. Chiprout, M. Nakhla, and Q. J. Zhang, "Analysis of high speed interconnects with frequency dependent parameters," in *Proc. Int. Symp. Electromag. Compat.,* Zurich, Switzerland, Mar. 1995, pp. 203–208.
[31] E. Chiprout and M. Nakhla, *Asymptotic Waveform Evaluation and Moment Matching for Interconnect Analysis.* Norwell, MA: Kluwer, 1993.
[32] D. Xie and M. Nakhla, "Delay and crosstalk simulation of high-speed VLSI interconnects with nonlinear terminations," *IEEE Trans. Computer-Aided Design,* vol. 12, pp. 1789–1811, Nov. 1993.
[33] C. R. Paul and S. A. Nasar, *Introduction to Electromagnetic Fields,* 2nd ed. New York: McGraw-Hill, 1987.
[34] C. W. Ho, A. E. Ruehli, and P. A. Brennan, "The modified nodal approach to network analysis," *IEEE Trans. Circuits Syst.*, vol. CAS-22, pp. 504–509, June 1975.
[35] G. A. Baker Jr., *Essential of Padé Approximants.* New York: Academic, 1975.
[36] J. H. McCabe, "A formal extension of the Padé table to include two point Padé quotients," *J. Inst. Math Applicat.,* vol. 15, pp. 363–372, 1975.
[37] P. Feldmann and R. W. Freund, "Efficient linear circuit analysis by Padé via Lanczos process," *IEEE Trans. Computer-Aided Design,* vol. 14, pp. 639–649, May 1995.
[38] A. R. Djordjević, T. K. Sarkar, and R. F. Harrington, "Time-domain response of multiconductor transmission lines," *Proc. IEEE,* vol. 75, pp. 743–764, June 1987.
[39] N. Gopal, D. P. Neikirk, and L. T. Pillage, "Evaluating on-chip *RC* interconnects using moment-matching approximations," in *Proc. IEEE Int. Conf. Computer-Aided Design,* Santa Clara, CA, 1991, pp. 74–77.

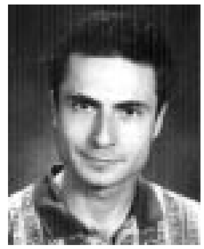

Roni Khazaka (S'92) received the B.E. and M.E. degrees from Carleton University, Ottawa, Ont., Canada, in 1995 and 1997, respectively, and is currently working toward the Ph.D. degree on the analysis and simulation of radio-frequency (RF) circuits.

His research interests include RF integrated circuits, circuit simulation, EM compatibility, and high-frequency interconnects.

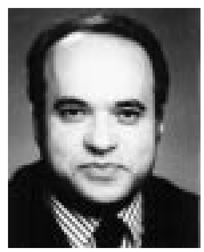

Michel S. Nakhla (S'73–M'75–SM'88–F"98) received the Ph.D. degree in electrical engineering from the University of Waterloo, Waterloo, Ont., Canada, in 1975.

From 1976 to 1988, he was with Bell-Northern Research, Ottawa, Ont., Canada, as the Senior Manager of the Computer-Aided Engineering Group. In 1988, he joined Carleton University, Ottawa, Ont., Canada, where he is currently a Professor in the Department of Electronics and Holder of the Computer-Aided Engineering Senior Industrial Chair established by Bell-Northern Research and the Natural Sciences and Engineering Research Council of Canada. He is the founder of the Computer-Aided Design (CAD) Research Group, Carleton University. He serves as Technical Consultant for several industrial organizations. He has authored or co-authored over 100 technical papers and two books on high-speed circuits and interconnects. His research interests include CAD of VLSI and communication systems, high-frequency interconnects, nonlinear simulation, synthesis of analog circuits, wavelets and neural networks.